जलवायु
JALAWAAYU
(Interdisciplinary Journal of Atmospheric and Hydrospheric Sciences)

Journal home page: https://cdhmtu.edu.np/journal/index.php/jalawaayu

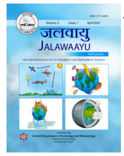

Type of paper: Original Article

Revisiting the 1993 Extreme Precipitation in Central Nepal: Synoptic Feature and Numerical Simulation

Binod Pokharel[1, 2], Kalpana Hamal[3, 4], Lin Zhao[2], Deepak Aryal[1], Dharmendra P. Rajbhandari[5], Suresh Marahatta[1, 6], and Shankar Sharma[1, *]

[1] Central Department of Hydrology and Meteorology, Tribhuvan University, Kirtipur Kathmandu, Nepal

[2] Utah Climate Center, Department of Plants, Soils, and Climate, Utah State University, Logan, UT, USA

[3] International Centre for Climate and Environment Sciences, Institute of Atmospheric Physics, Chinese Academy of Sciences, P.O. Box 9804, Beijing 100029, China

[4] University of Chinese Academy of Sciences, Beijing 100049, China

[5] Department of Meteorology, Tri-Chandra Campus, Tribhuvan University, Kathmandu, Nepal

[6] RECHAM Consult Pvt. Ltd., Putalisadak, Kathmandu, Nepal

ARTICLE INFO

Received: 18 February 2022
Received in Revised form: 07 March 2022
Accepted: 14 April 2022
Available Online: 31 May 2022

Keywords

Extreme precipitation
WRF
Nepal
Simulations

**Correspondence*
Shankar Sharma
E-mail: sharma.sh969@gmail.com

Abstract: The cloudburst event occurred on 19-20 July 1993, created a devastating flash flood over south-central Nepal. The storm killed hundreds of people, and damaged millions of dollars of properties. This study focused on the synoptic and thermodynamics that triggered the cloudburst in central Nepal, bringing 540 mm of rainfall over a small region in less than 24 hours. Moreover, it investigates the primary reason for the particular extremest event in Nepal. Our results show the strong upward motion transported the significant moisture that led to favorable condition for development of thick cloud cover, producing a record-breaking precipitation during that event over central Nepal. Likewise, the monsoon trough with negative sea level pressure anomaly over central Nepal located east of the upper-level trough further suggests a westward tilt with

Cite this paper: Pokharel, B., Hamal, K. ., Zhao, L., Aryal, D. ., Rajbhandari, D. P. ., Marahatta, S. ., & Sharma, S. Revisiting the 1993 Extreme Precipitation in Central Nepal: Synoptic Feature and Numerical Simulation. Jalawaayu, 2(1), 33–44. https://doi.org/10.3126/jalawaayu.v2i1.45392

height in the disturbances associated with cloudburst on the event day. Further, we also simulate the extreme precipitation events over the region using Weather Research Forecast (WRF) model however, it underestimated the precipitation amount with slight shift in event location. The model simulates the actual thermodynamics, but it fails to produce the actual precipitation. Moreover, it is difficult to simulate the actual topography over the complex region where orography plays an essential role in producing high precipitation.

1. Introduction

South Asian monsoon brings a significant amount of precipitation during the summer season (June-September), and some extreme events are common every year in South Asia (Sharma *et al.*, 2020b; Talchabhadel *et al.*, 2020), where the world's tallest clouds of deep convection form (Houze Jr *et al.*, 2007; Rasmussen and Houze Jr, 2012). Nepal has witnessed several of them during the monsoon season (Sharma *et al.*, 2020b; Karki *et al.*, 2017; Talchabhadel *et al.*, 2018). Such extreme precipitation usually brings flash floods and/or long-duration floods, landslides, and debris flows. However, the 1993 extreme precipitation in Nepal occurred over a small area with a cloudburst that brought the flash flood, killed 1336 people, destroyed 17,113 houses, damaged Kulekhani hydroelectric project (92MW), major highways and bridges, and caused $34 million in property loss (Yogacharya and Gautam, 2008). The event happened by abnormal behavior of monsoon depression paths originating from the Bay of Bengal when associated with the low-pressure center in Nepal. Extreme precipitation forecasting is difficult as weather forecasting models either feature high resolution or do not capture extreme precipitation with spatial accuracy (Talchabhadel *et al.*, 2022). The forecasting skill during the 1990s was very poor or even almost no weather forecasting period. The poor weather forecasting and limited observational data make it difficult to get an early warning for the people affected by the extreme precipitation (Sillmann *et al.*, 2017). Even though a high-resolution WRF model has been run for weather forecasting in Nepal, the model has several limitations regarding the timing, location, and precipitation forecasting accuracy. This worsens when cloud burst events occur during the summer monsoon within a small area where topography plays an important role in downburst heavy precipitation within a few hours.

The extreme event on 19 and 20 July 1993 brought 540 mm of rainfall within less than 24 hours (Figure 1) (Marahatta and Bhusal, 2009). The event was left without a detailed study of the synoptic and mesoscale phenomenon that brought record-breaking one-day precipitation in central Nepal. This study analyzes the detailed synoptic/mesoscale phenomenon that generated the cloud burst in central Nepal (now in Bagmati Province). Central Nepal (between 83^{o}E and 86^{o}E) received the four highest rainfall events of more than 400 mm/day, including the July 1993 event and the 10 highest rainfall events among the top 15 heaviest rainfall in all of Nepal (Shrestha, 2016). However, these extreme events are shifting all over Nepal, mainly during the last decades (Karki *et al.*, 2017). Measuring these extreme events is important to understand the precipitation mechanisms and relay a timely warning to the settlements in hillside and downstream locations. The satellite and remote sensing estimations of extreme precipitation are far from accurate, underestimating the actual precipitation by 30 to

80% (Shrestha *et al.*, 2021; Talchabhadel *et al.*, 2021). Even though more satellite remote sensing precipitation sensors are available however, these satellite measurements are indirect measurement, which may provide spatial and temporal accuracy (Sharma *et al.*, 2020a). Thus, denser ground-based measurements are needed to capture the spatial distribution of highly variable precipitation fields in the complex topography of Nepal.

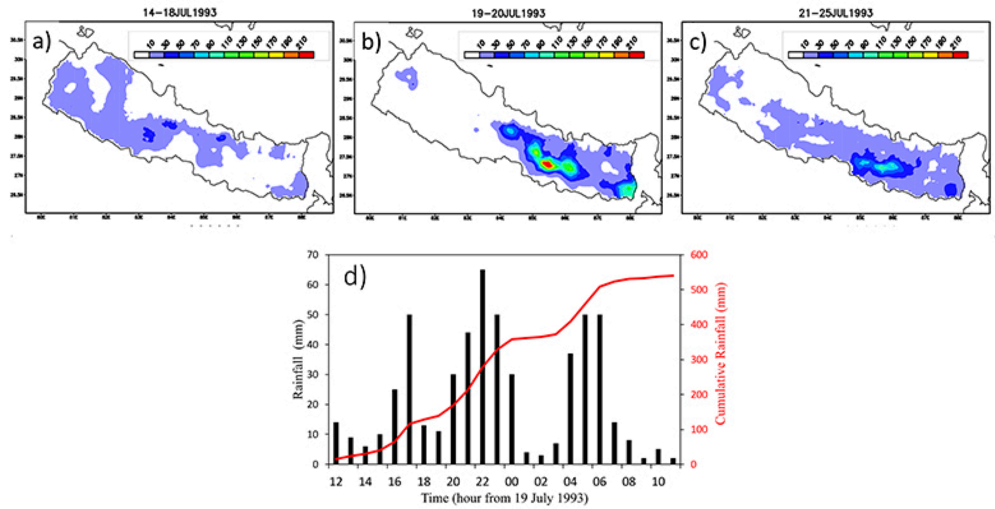

Figure 1. Aphrodite precipitation during (a) 14–18 July 1993, (b) 19–20 July 1993, and (c) 21-25 July 1993, and (d) hourly cumulative rainfall from 19 July 1993.

2. Materials and Methods

2.1 Study area and datasets

We considered the high-resolution APHRODITE precipitation data to analyze the high-precipitation region during the extreme precipitation event. We considered the National Centers for Environmental Prediction (NCEP-1) including upper level and surface synoptic records for the current study (Kalnay *et al.*, 1996). The NCEP/NCAR Reanalysis 1 project is using a state-of-the-art analysis/forecast system to perform data assimilation using past data from 1948 to the present. For the upper and lower levels atmospheric condition, we have selected the NCEP data at pressure level of 200, 500 and 700 hPa. The precipitation distribution during the extreme precipitation event, before (10 days), and after the extreme event on 19-20 July 1993 was also considered.

2.2 WRF Model setup

The WRF was continuously updated, and version 3.8.1 of WRF (Skamarock, 2008) was utilized in this study (Figure 2). Three domains with a grid spacing of 27 (d01), 9 (d02), and 3 km (d03), were configured for the WRF simulation for extreme precipitation event (Figure 2). The motive behind simulating the WRF is to analyze whether the weather model can reproduce extreme weather event. The forcing data used to run the WRF model is Climate Forecast System Reanalysis (CFSR). The WRF model was simulated considering four different microphysics schemes with the same boundary layer and other schemes (Table 1).

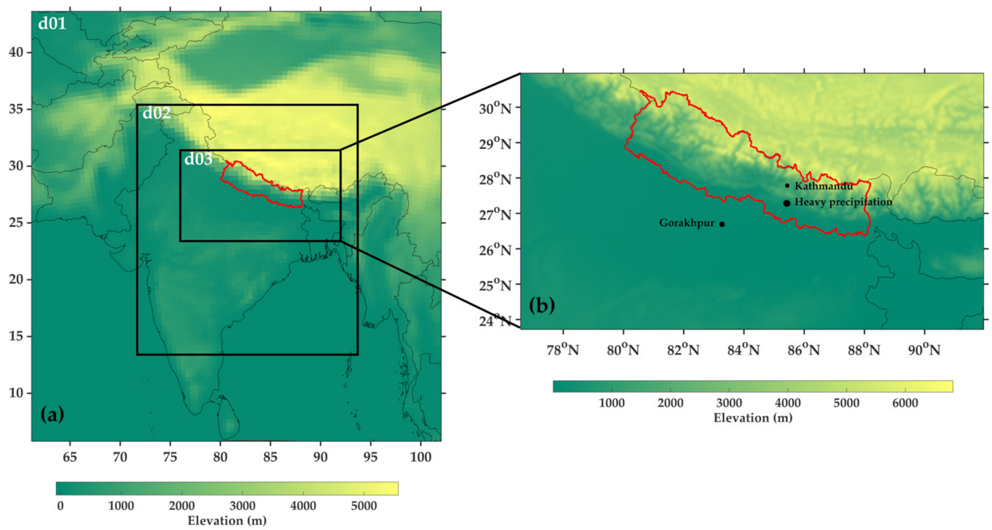

Figure 2. Study domain in the WRF, (a) Inner domain 3km (d03), outer domain 10km (d02), outermost domain 50km (d01). (b) Heavy precipitation location in Nepal.

The innermost domain was centered on Nepal, where the extreme precipitation occurred on 19–20 July 1993. The land use/land cover and topography driven data from the U.S. Geological Survey (USGS) were set at 2 min spatial resolution for d01 and d02, and d03. The simulations of the three domains were all initiated at 00 UTC 14 June 2010 with an integration time span of 6 h and the model spin-up time of about 3 h (d01) and 1 h (d02 and d03). The main physical parameterization schemes for the simulations are listed in Table 1.

Table 1. Summary table of the WRM run to simulate the extreme event of 19-20 July 1993

Variables	Physics options	LCL pressure, hPa	LCL temp, ^{0}C	PW, mm	CAPE, J/kg
Observed		809	19	4	2907
WRF (1st run)	WSM 6-class graupel	895	22	6	1550
WRF (2nd run)	Lin et al.	894	22	6	1799
WRF (3rd run)	Ferrier scheme	911	23	6	0
WRF (4th run)	Thompson graupel	896	22	6	1978

3. Results and discussion

3.1 Synoptic environment for extreme event

We first analyzed the upper and lower-level synoptic conditions using wind vorticity during 19–20 July 1993 (Figure 3). The upper level, slowly moving through (200 mb), was located in the western Himalayas until 18 July (Figure 3a). The trough moved to the central Himalayas on 19 July with a much deeper wave that produced strong positive vorticity over Tibet and upper-level divergence around central/eastern Nepal (Figure 3b). The upper-level trough is well connected with mid-level circulation (500 mb) with strong positive vorticity is located exactly over central/eastern Nepal, where extreme precipitation occurred (Figure 3d). It is worth mentioning that the mid-level trough was in the south of Nepal for more than 10 days (Figure 3c), with two strong vorticity zones on India's east and west coasts with negative vorticity over Nepal. The strong trough-ridge-trough pattern developed, and positive vorticity moved to eastern-central Nepal during extreme precipitation on 19-20 July (Figures 3b and e). After the extreme event, the ridge pattern is developed over the central Himalayas in the upper and middle atmosphere (Figures 3c and f).

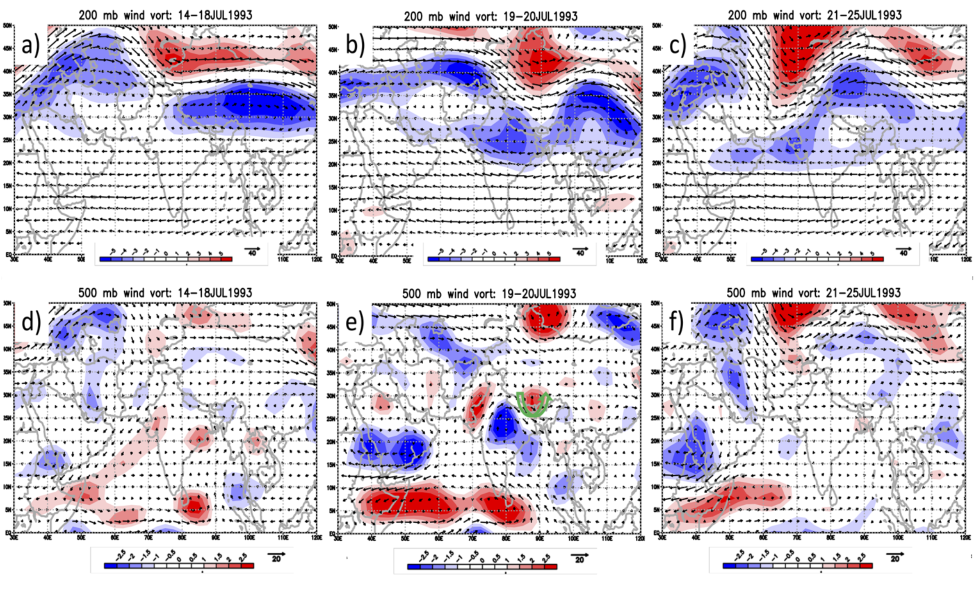

Figure 3. The upper and mid-level vorticity wind during (a, d) 14–18 July 1993, (b, e) 19–20 July 1993, and (c, d) 21-25 July 1993.

We further diagnosed the lower atmosphere considering 700 mb and surface conditions before, during, and after the extreme events (Figure 4). It is observed that the lower and middle atmosphere is well connected with strong positive vorticity located over northern India and negative vorticity in Nepal for about 10-days (Figure 4a) before the extreme event. The deeper trough-ridge pattern developed during 19-20 July with strong positive vorticity just over the extreme precipitation region (Figure

4b). That strong positive-negative vorticity dipole type pattern diminished after the extreme event (Figure 4c). The extreme precipitation environment was supported by the surface-atmosphere shown by the sea level pressure contour plots (Figure 4d-f). During the earlier period, the monsoon trough located in the south of Nepal (Figure 4d) was parallel with the Himalayas. However, the trough is tilted with the eastern edge slightly moved to the north entering central Nepal (Figure 4e) during the extreme precipitation event on 19-20 July. This led to extreme precipitation when the monsoon trough was slightly moved/entered Nepal. The deep trough helps in moisture transport from the Bay of Bengal and contributes to the heavy rainfall development (Sadaf *et al.*, 2021). The monsoon trough changed its position remaining in the south of Nepal again after the extreme event (Figure 4f).

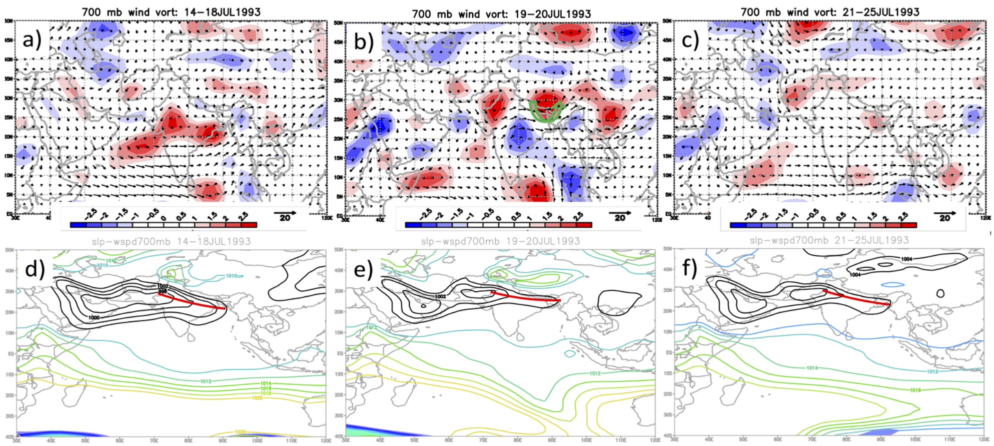

Figure 4. The lower-level vorticity wind and sea level pressure during (a, d) 14-18 July 1993, (b, e) 19-20 July 1993, and (c, f) 21-25 July 1993. Red line in panel d, e, and f represents the trough.

3.2 Thermodynamics

3.2.1 Moisture flux transport and sounding

We have further analyzed the thermodynamics environment using the moisture and nearest sounding data (Figure 5). The closest sounding during that time was Gorakhpur, India (Figure 1), which was released on 00Z 20 July (5:45 am Nepal time). Although the sounding location was not around the area with strong positive vorticity and moisture convergence zone, it showed strong instability (CAPE ~3000 J/kg) even in the early morning (Figure 5), favoring extreme precipitation conditions over Nepal.

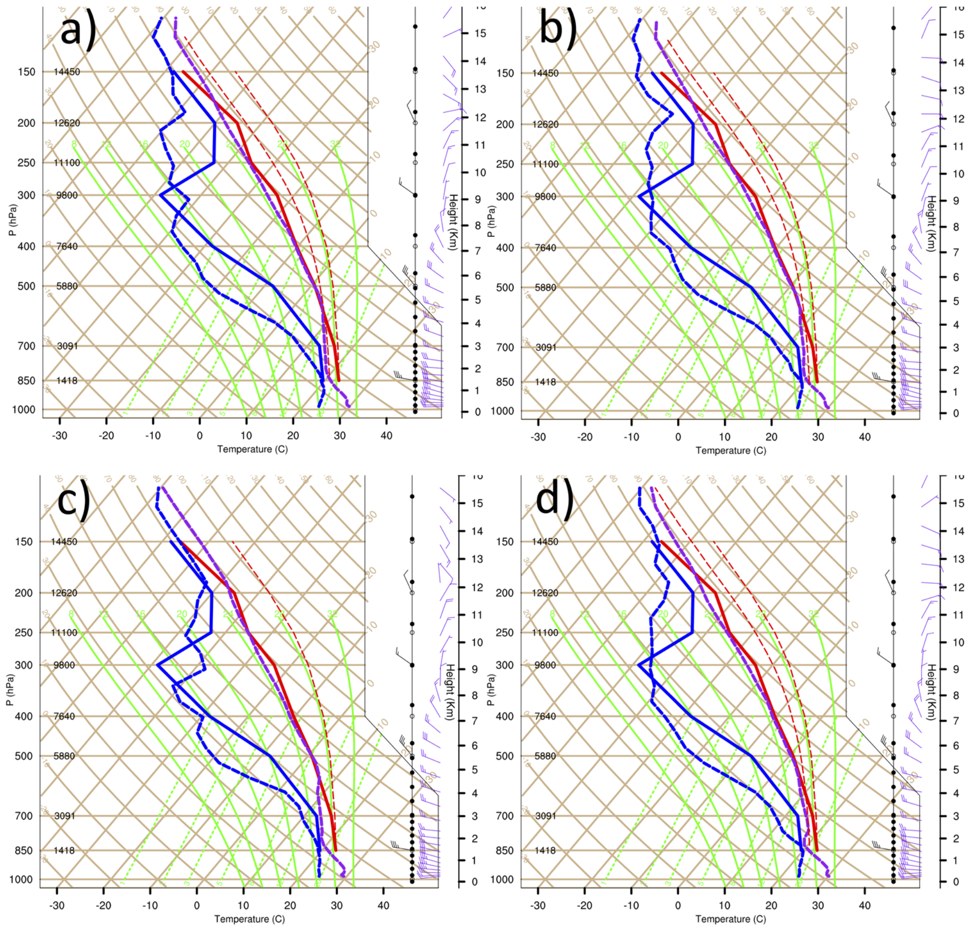

Figure 5. Pressure and temperature recorded in the sounding of the Gorakhpur stations.

We also looked at the vertically integrated moisture flux before, during, and after the extreme event (Figure 6). The positive moisture flux (convergence) is observed over the south from Nepal (north India) and Tibetan Plateau for more than a weak (Figure 6a). The moisture flux is consistent with the vorticity, and strong moisture convergence was over the extreme precipitation region in central and eastern Nepal during the cloud burst (Figure 6b). The southerly flow of warm and moist air from the Bay of Bengal is enhanced and thus creates a high moisture transport to Nepal (Hamal *et al.*, 2021; Sharma *et al.*, 2020b). Further, after extreme precipitation, the moisture flux significantly decreased significantly in Nepal (Figure 6c).

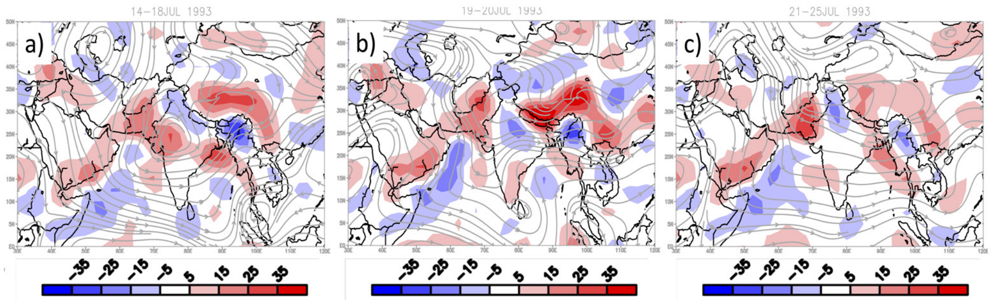

Figure 6. The vertically integrated moisture flux during (a) 14-18 July 1993, (b) 19-20 July 1993, and (c) 21-25 July 1993.

3.3 WRF model simulation

We simulated the extreme event on 19-20 July 1993 using the WRF model, and the spatial distribution of different runs is presented in Figure 7. Even though the coarse resolution reanalysis data captured the synoptic condition well, the high-resolution WRF model could not produce the precipitation. We used four different microphysics schemes (Table 1) widely used to simulate extreme precipitation but could not produce the actual amount of precipitation. However, all simulations produced a higher amount of precipitation around the location where extreme precipitation occurred (Figure 7a-c). The result shows that the WRF model has limited skill in reproducing the extreme precipitation of 19-20 July. Further, the abilities of the WRF simulation to simulate precipitation over Nepal are highly dependent on their ability to express the dynamical and thermal effects of complex terrain at different horizontal scales (Palazzi *et al.*, 2013; Ma *et al.*, 2009). Such physical and thermal effects may be related to the dynamical core, sub-grid scale physical parameterizations, and horizontal resolutions during model configuration. Furthermore, the sub-grid scale and orographic drag scheme significantly modulate the atmospheric circulation and local land-atmosphere interactions (Zhang *et al.*, 2006; Zhou *et al.*, 2017; Zhou *et al.*, 2018). The cumulus convection scheme directly modifies the convective precipitation within one grid cell; on the other hand, the high-resolution simulations can resolve more orography and yield better results than low-resolution simulations (Lin *et al.*, 2018). Overall, the topographical influence can reduce the griding spacing, impacting the model's performance (Ouyang *et al.*, 2021).

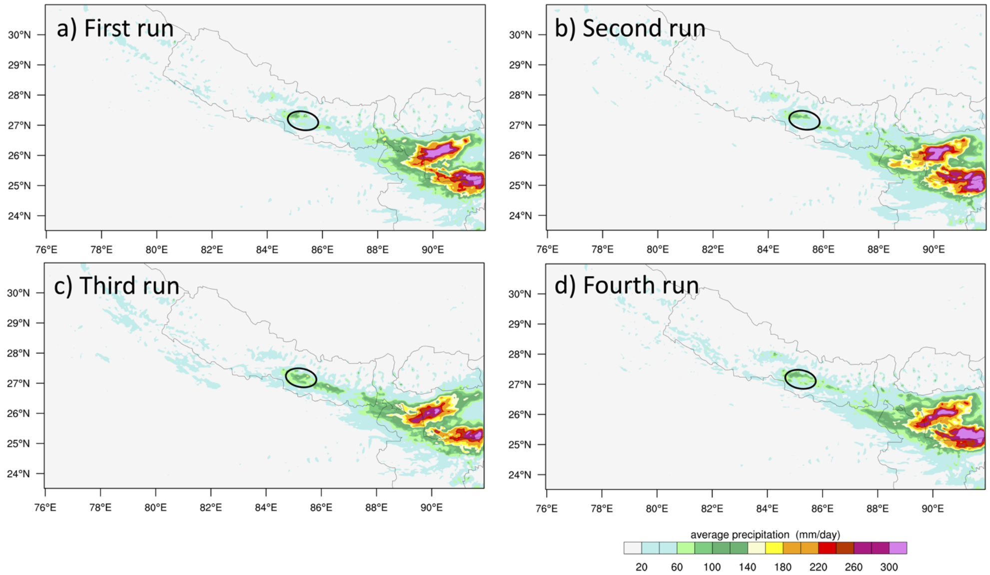

Figure 7. WRF simulation of four microphysics (a) first run (WSM 6-class graupel), (b) second run (Lin et al), (c) third run (Ferrier scheme), and (d) fourth run (Thompson graupel) over Nepal during the extreme event on 19-20 July 1993. The black circle represents the heavy precipitation events.

4. Summary and Conclusion

The storm environment of extreme precipitation on 19-20 July 1993 is studied using multiple datasets. In addition, the WRF model is run to simulate the extreme precipitation and associated thermodynamics. The extreme precipitation in central Nepal produced 540 mm of rainfall in less than 24 hours. The cloudburst event produced flash floods in Bagmati and other Rivers that destroyed significant highways, bridges, and irrigation dams. Extreme precipitation occurred in a well-setting synoptic environment with strong positive vorticity up to 500 mb and high moisture flux. The strong upward motion transported the moisture, creating an intense cloud over the region, producing record-breaking precipitation during that event. The monsoon trough and negative SLP anomaly over central Nepal located east of the upper-level trough suggests a westward tilt with height in the disturbances associated with cloudburst on that day.

Further, the WRF model could not simulate the precipitation over the region, but it produced higher precipitation around the same location. The model simulates the actual thermodynamics, but it fails to produce the actual precipitation. It is not easy to simulate the actual topography over the complex region where orography plays an essential role in producing high precipitation.

Acknowledgments: This research is supported by the Research Grants to Faculty Appointed through Research Excellence based Open Competition Under the Higher Education Reforms Project (HERP DLI-7B). We highly acknowledge the scientist of National Center for Environmental Prediction for providing NCEP data freely.

Conflicts of Interest: The authors declare no conflict of interest.

References

Hamal, K., Sharma, S., Pokharel, B., Shrestha, D., Talchabhadel, R., Shrestha, A. and Khadka, N. (2021) Changing pattern of drought in Nepal and associated atmospheric circulation. *Atmospheric Research,* **262**: 105798.

Houze Jr, R. A., Wilton, D. C. and Smull, B. F. (2007) Monsoon convection in the Himalayan region as seen by the TRMM Precipitation Radar. *Quarterly Journal of the Royal Meteorological Society: A journal of the atmospheric sciences, applied meteorology and physical oceanography,* **133**: 1389-1411.

Kalnay, E., Kanamitsu, M., Kistler, R., Collins, W., Deaven, D., Gandin, L., Iredell, M., Saha, S., White, G. and Woollen, J. (1996) The NCEP/NCAR 40-year reanalysis project. *Bulletin of the American Meteorological Society,* **77**: 437-472.

Karki, R., Schickhoff, U., Scholten, T. and Böhner, J. (2017) Rising precipitation extremes across Nepal. *Climate,* **5**: 4. https://doi.org/10.3390/cli5010004

Lin, C. G., Chen, D. L., Yang, K. and Ou, T. H. (2018) Impact of model resolution on simulating the water vapor transport through the central Himalayas: implication for models' wet bias over the Tibetan Plateau. *Climate Dynamics*. 10.1007/s00382-018-4074-x

Ma, L., Zhang, T., Frauenfeld, O. W., Ye, B., Yang, D. and Qin, D. (2009) Evaluation of precipitation from the ERA-40, NCEP-1, and NCEP-2 Reanalyses and CMAP-1, CMAP-2, and GPCP-2 with ground-based measurements in China. *Journal of Geophysical Research: Atmospheres,* **114**.

Marahatta, S. and Bhusal, J. K. (2009) Relating hydrological extremes with area-A case on extreme floods in South Central Nepal. *Journal of Hydrology and Meteorology,* **6**: 44-48.

Ouyang, L., Lu, H., Yang, K., Leung, L. R., Wang, Y., Zhao, L., Zhou, X., Chen, Y., Jiang, Y. and Yao, X. (2021) Characterizing Uncertainties in Ground "Truth" of Precipitation Over Complex Terrain Through High-Resolution Numerical Modeling. *Geophysical Research Letters,* **48**: e2020GL091950.

Palazzi, E., von Hardenberg, J. and Provenzale, A. (2013) Precipitation in the Hindu-Kush Karakoram Himalaya: Observations and future scenarios. *Journal of Geophysical Research-Atmospheres,* **118**: 85-100. 10.1029/2012jd018697

Rasmussen, K. L. and Houze Jr, R. A. (2012) A flash-flooding storm at the steep edge of high terrain: disaster in the Himalayas. *Bulletin of the American Meteorological Society,* **93**: 1713-1724.

Sadaf, N., Lin, Y. and Dong, W. (2021) Wet spells over the core monsoon domain of northern Pakistan during the summer season. *International Journal of Climatology,* **41**: 1402-1420.

Sharma, S., Chen, Y., Zhou, X., Yang, K., Li, X., Niu, X., Hu, X. and Khadka, N. (2020a) Evaluation of GPM-Era Satellite Precipitation Products on the Southern Slopes of the Central Himalayas Against Rain Gauge Data. *Remote Sensing,* **12**: 1836. 10.3390/rs12111836

Sharma, S., Hamal, K., Khadka, N. and Joshi, B. B. (2020b) Dominant pattern of year-to-year variability of summer precipitation in Nepal during 1987–2015. *Theoretical and Applied Climatology,* **142**: 1071-1084. 10.1007/s00704-020-03359-1

Shrestha, A. 2016. *Cloudbursts in the Nepal Himalayas: Interaction between the Indian monsoon and extratropics,* The University of Wisconsin-Madison.

Shrestha, D., Sharma, S., Talchabhadel, R., Deshar, R., Hamal, K., Khadka, N. and Nakamura, K. (2021) Detection of Spatial Rainfall Variation over the Andean Region Demonstrated by Satellite-Based Observations. *Atmosphere,* **12**: 1204.

Sillmann, J., Thorarinsdottir, T., Keenlyside, N., Schaller, N., Alexander, L. V., Hegerl, G., Seneviratne, S. I., Vautard, R., Zhang, X. and Zwiers, F. W. (2017) Understanding, modeling and predicting weather and climate extremes: Challenges and opportunities. *Weather and climate extremes*, **18**: 65-74.

Skamarock, W. (2008) A description of the advanced research WRF version 3. NCAR Technical Note TN-475+ STR. *National Center for Atmospheric Research.[Available online at https://www2. mmm. ucar. edu/wrf/users/docs/technote/v3\technote. pdf]*.

Talchabhadel, R., Aryal, A., Kawaike, K., Yamanoi, K. and Nakagawa, H. (2020) A comprehensive analysis of projected changes of extreme precipitation indices in West Rapti River basin, Nepal under changing climate. *International Journal of Climatology*.

Talchabhadel, R., Karki, R., Thapa, B. R., Maharjan, M. and Parajuli, B. (2018) Spatio-temporal variability of extreme precipitation in Nepal. *International Journal of Climatology*, **38**: 4296-4313. https://doi.org/10.1002/joc.5669

Talchabhadel, R., Nakagawa, H., Kawaike, K., Yamanoi, K., Musumari, H., Adhikari, T. R. and Prajapati, R. (2021) Appraising the potential of using satellite-based rainfall estimates for evaluating extreme precipitation: A case study of august 2014 event across the west rapti river basin, Nepal. *Earth and Space Science*, **8**: e2020EA001518.

Talchabhadel, R., Sharma, S., Khadka, N., Hamal, K., Karki, S. and Thapa, B. R. (2022) An outlook on the applicability of satellite precipitation products for monitoring extreme precipitation events in Nepal Himalaya. *Weather*.

Yogacharya, K. S. and Gautam, D. K. 2008. Floods in Nepal: Genesis, Magnitude, Frequency and Consequences. Kathmandu: Society of Hydrologists and Meteorologists-Nepal.

Zhang, Y. C., Huang, A. N. and Zhu, X. S. (2006) Parameterization of the thermal impacts of sub-grid orography on numerical modeling of the surface energy budget over East Asia. *Theoretical and Applied Climatology*, **86**: 201-214. 10.1007/s00704-005-0209-1

Zhou, X., Beljaars, A. C. M., Wang, Y., Huang, B., Lin, C., Chen, Y. and Wu, H. (2017) Evaluation of WRF Simulations with Different Selections of Sub-grid Orographic Drag over the Tibetan Plateau. *Journal of Geophysical Research-Atmospheres*, **122**: 7755-7771. 10.1002/2016JD026213

Zhou, X., Yang, K. and Wang, Y. (2018) Implementation of a turbulent orographic form drag scheme in WRF and its application to the Tibetan Plateau. *Climate Dynamics*, **50**: 2243-2255. 10.1007/s00382-017-3677-y